ACS APPLIED POLYMER MATERIALS

pubs.acs.org/acsapm Article

Utilizing a Fluorinated Derivative as a Dual-Function Modifier to Improve the Interface Engineering and Long-Term Stability of Inverted Perovskite Solar Cells

Yuanlin Yang, Ying Li, Yanqing Yao, Xusheng Zhao, Siwen Wu, Ling Qin, Xiude Yang, Ping Li,* and Lijia Chen*

Cite This: ACS Appl. Polym. Mater. 2024, 6, 10254−10262 Read Online

ACCESS | Metrics & More | Article Recommendations | Supporting Information

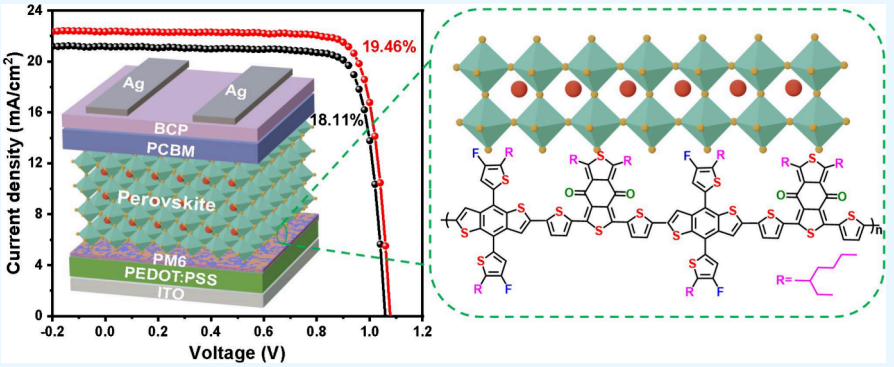

ABSTRACT: Poly(3,4-ethylenedioxythiophene):poly(styrenesulfonate) (PEDOT:PSS) is a frequently used hole transport layer (HTL) that often constrains the stability and efficiency of inverted perovskite solar cells (PSCs) because of its hydrophilic properties. In the study, a hydrophobic fluorinated derivative (PM6) was employed as an interfacial modifier for the PEDOT:PSS layer. Modification with PM6 improved the hydrophobicity and work function (WF) of the PEDOT:PSS and mitigated the formation of charge recombination centers (Pb^0) on the perovskite surface. The improvement reduced energy losses at the interface by facilitating hole extraction and transport across the PEDOT:PSS/perovskite interface. The PSCs incorporating PM6-modified PEDOT:PSS demonstrated a power conversion efficiency (PCE) of 19.46%, superior to the 18.11% PCE observed for cells utilizing the unmodified PEDOT:PSS. Moreover, the PSCs were subjected to temperature conditions (25 °C) and 15% relative humidity for a period of 360 h. The PM6-modified PEDOT:PSS device maintained 89.75% of its initial PCE. In contrast, the PCE of the pristine device had dropped to 75.06% of its initial PCE. Thus, the PM6-based modification of the PEDOT:PSS/perovskite interface emerges as a viable strategy to bolster the performance and reliability of inverted PSCs.

KEYWORDS: *PEDOT:PSS, PM6, hole transport layer, inverted perovskite solar cells, long-term stability*

1. INTRODUCTION

Inverted perovskite solar cells (PSCs) are widely recognized as a highly promising advancement in solar cell technology due to their exceptional spectral absorption, cost-effectiveness in fabrication, adaptable composition, superior structural integrity, and remarkable optoelectronic properties.[1−6] However, PEDOT:PSS, a commonly utilized material as a hole transport layer (HTL) in inverted PSCs,[7] contains poly(styrenesulfonate) (PSS), which is a water-soluble polymer with strong hydrophilicity.[8] Consequently, when exposed to humid environments, PEDOT:PSS absorbs moisture from its surroundings, leading to moisture transfer to the perovskite upon contact, which accelerates the degradation of the perovskite at the PEDOT:PSS/perovskite interface, thereby shortening the lifespan of the device. Moreover, perovskite degradation can result in the formation of charge recombination defects and energy losses at the interface, significantly impacting device efficiency.[9,10] Therefore, to enhance the device efficiency and environmental stability of PSCs, it is imperative to mitigate losses caused by PEDOT:PSS and the PEDOT:PSS/perovskite interface.[11,12]

Recent studies have pinpointed the hydrophilic nature and interface defects of PEDOT:PSS as the primary factors contributing to both low device stability and reduced

Received: April 29, 2024
Revised: August 1, 2024
Accepted: August 5, 2024
Published: August 27, 2024

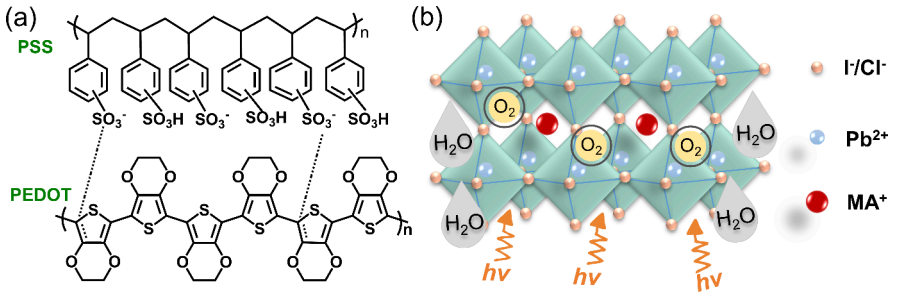

Figure 1. (a) Molecular structure of the PEDOT:PSS. (b) Factors influencing perovskite stability: water, oxygen, and light.

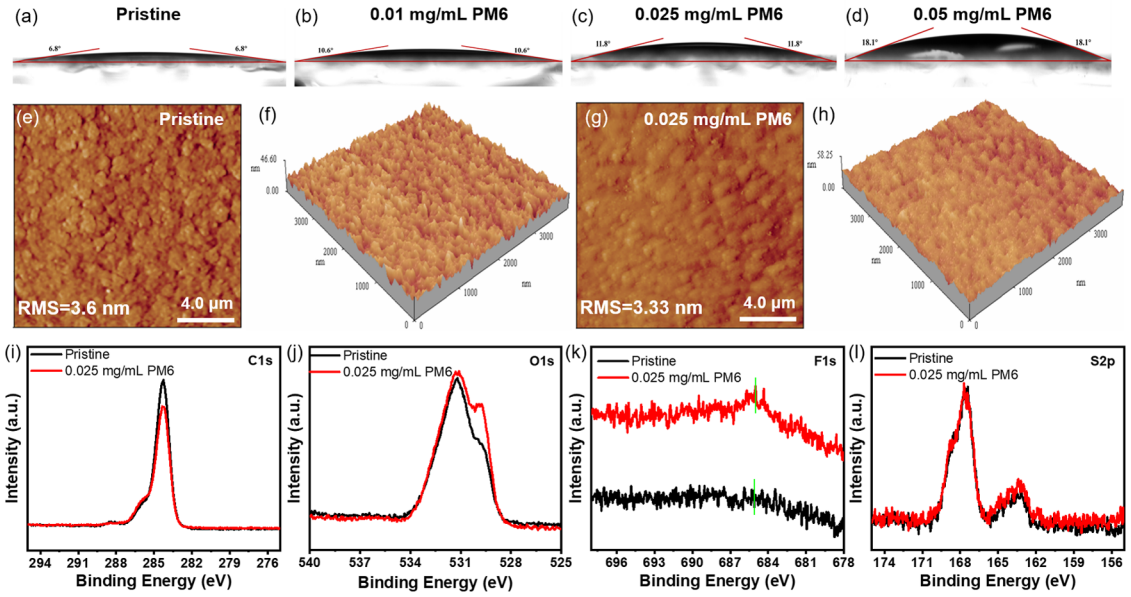

Figure 2. Contact angles of the PEDOT:PSS films modified with different concentrations of PM6: (a) pristine, (b) 0.01 mg/mL PM6, (c) 0.025 mg/mL PM6, and (d) 0.05 mg/mL PM6. AFM images of different HTL films: (e) 2D and (f) 3D of pristine and (g) 2D and (h) 3D of 0.025 mg/mL PM6. The XPS characterization of (i) C 1s orbitals, (j) O 1s orbitals, (k) F 1s orbitals, and (l) S 2p orbitals in pristine and 0.025 mg/mL PM6 films.

photovoltaic efficiency.[13,14] To address the hydrophilicity of PEDOT:PSS, Wang et al.[15] introduced an ultrathin layer of poly(triarylamine) (PTAA) onto PEDOT:PSS, achieving a PCE of 19.04%. After storage under ambient conditions for 250 h, the PCE of the PSCs with the PTAA modification is still maintained at the 90% level, indicating significantly improved stability. However, the valence band mismatch between the PEDOT:PSS layer and the perovskite layer creates a contact barrier at the interface. Al-Gamal et al.[16] introduced a layer of ethylenediamine-functionalized graphene (EDA-FG) between the indium tin oxide (ITO) and PEDOT:PSS, forming a bilayer hole transport structure. The EDA-FG modification reduced energy losses at the PEDOT:PSS/perovskite interface, resulting in an increase in the PCE of the device from 13.71% to 17.66%. In addition to the aforementioned modification materials, the polymer donor material PM6 exhibits significant advantages, including high hole mobility, hydrophobic properties, and the ability to passivate defects in the perovskite films, making it widely applicable in PSCs.[17,18] When PM6 is used as an HTL instead of spiro-OMeTAD (with a PCE of 14.46%), it significantly improves the optoelectronic performance of the PSCs (with a PCE of 16.06%).[18] It is worth noting that currently no research group has applied PM6 to inverted PSCs, particularly for modifying the PEDOT:PSS/perovskite interface.

In the study, we applied a layer of PM6 to modify PEDOT:PSS in order to enhance its hydrophilic properties and passivate charge recombination centers on the perovskite film surface. The PM6 modification effectively suppresses charge recombination and promotes charge transport at the PEDOT:PSS/perovskite interface, thereby reducing the energy losses. The results demonstrate that PSCs modified with PM6 show an increase in open-circuit voltage (V_{oc}) from 1.04 to 1.06 V and a boost in PCE from 18.11% to 19.41%. Furthermore, even after storage under air conditions (25 °C at RH 15%) for 360 h, the PCE of the PSCs modified with PM6 remains at the 89.75% level, indicating significantly enhanced stability. Consequently, PM6 emerges as a promising material for interface modification, showcasing its effectiveness in improving both the PCE and stability in PSCs. Introducing a PM6 modification layer at the PEDOT:PSS/perovskite interface represents a viable strategy for enhancing the performance of PSCs.

2. RESULTS AND DISCUSSION

PEDOT:PSS is a copolymer consisting of poly(3,4-ethylenedioxythiophene) (PEDOT) and PSS. PEDOT is an organic

https://doi.org/10.1021/acsapm.4c01309
ACS Appl. Polym. Mater. 2024, 6, 10254−10262

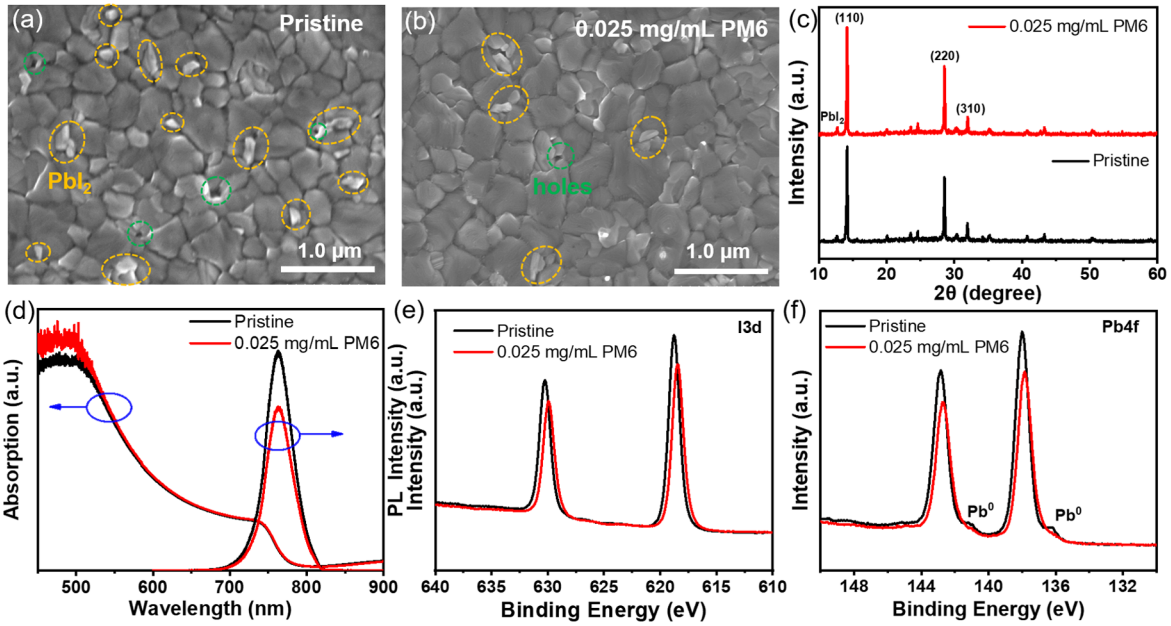

Figure 3. SEM morphology of perovskite films deposited on (a) pristine and (b) 0.025 mg/mL PM6. (c) XRD diffractograms and (d) absorption and PL spectra of chalcogenide films deposited on pristine and 0.025 mg/mL PM6. XPS characterization of (e) I 3d and (f) Pb 4f orbitals in pristine encapsulated and PM6/encapsulated films.

semiconductor material renowned for its excellent electrical conductivity and optoelectronic properties. Conversely, PSS is a negatively charged polymer that enhances the solubility and stability of PEDOT. The molecular structure is depicted in Figure 1a. Moreover, due to the perovskite materials vulnerability to environmental factors such as water, oxygen, and light, they are prone to decomposing into defects like PbI_2 and Pb^0,[19−21] as illustrated in Figure 1b. Consequently, the study proposes the modification of PEDOT:PSS with PM6 to address the instability issue in ITO/PEDOT:PSS/MAPbI$_{3-x}$Cl$_x$/PCBM/BCP/Ag structured PSCs.

$$CH_3NH_3PbI_{3-x}Cl_x \rightarrow PbI_2 + CH_3NH_2 + I_2\uparrow + Cl_2\uparrow + H_2\uparrow \quad (1)$$

$$PbI_2 \rightarrow Pb^0 + I_2\uparrow \quad (2)$$

To investigate the hydrophobicity of PEDOT:PSS modified with various concentrations of PM6, we conducted tests to measure the surface water contact angle after applying different concentrations of PM6 to PEDOT:PSS. As shown in Figures 2a−2d, there is a clear positive correlation between the water contact angle and the concentration of PM6. When PM6 is modified in PEDOT:PSS, the water contact angle increases correspondingly with the increase in PM6 concentration, rising from 6.8° to 18.1°. This indicates that at equivalent spinning speeds higher concentrations of PM6 result in greater hydrophobicity of the PEDOT:PSS/PM6 film. The PM6 modification enhances hydrophobicity, which helps mitigate the hydrophilic nature of PEDOT:PSS and its adverse effects on the perovskite film, thereby alleviating perovskite film degradation. As a result, it improves the humidity stability of PSCs.[22] However, while a higher water contact angle signifies improved hydrophobicity of the HTL, excessively high water contact angles can impede the deposition of the perovskite film, resulting in inferior film quality. The finding emphasizes the importance of employing an appropriate amount of PM6 to optimize interface properties and achieve superior perovskite film quality and performance.

The surface smoothness of the HTL is crucial in determining the quality of deposited perovskite films, with lower surface roughness favoring the formation of high-quality perovskite films.[23] Thus, AFM analysis was carried out to investigate the surface morphology of the films at varying PM6 concentrations. As illustrated in Figures S1a−S1d, the surface roughness of the PEDOT:PSS film measures 3.6 nm. However, the roughness of PM6 films at different concentrations is notably reduced, with the 0.025 mg/mL PM6 film showing the lowest roughness (RMS = 3.33 nm), as shown in Figures 2e−2h. This smoother surface facilitates the deposition of high-quality perovskite films.

The chemical states of C 1s, O 1s, F 1s, and S 2p on the surface of ITO/PEDOT:PSS/PM6 films were characterized by using XPS analysis in order to investigate the effect of PM6 on the surface chemical composition of PEDOT:PSS films. As illustrated in Figures 2i−2l, the C 1s orbital spectra reveal a prominent peak at 284.80 eV (C−C/C−H) and 286.35 eV (C−O) in the pristine film. Conversely, in the 0.025 mg/mL PM6 film, the characteristic peaks are positioned at 284.79 eV (C−C/C−H) and 286.40 eV (C−O), indicating a red shift of 0.05 eV in the characteristic peak representing the C−O bond in PM6-modified PEDOT:PSS. In the O 1s orbital spectra, the characteristic peaks of the C−O bond detected in the pristine film and the 0.025 mg/mL PM6 film are situated at 531.71 and 531.58 eV, respectively. Meanwhile, the peaks of the C═O bond are located at 530.00 and 530.20 eV, respectively. Consequently, after PM6 coating, the characteristic peaks of the C═O bond undergo a red shift, indicating the interaction between PEDOT:PSS and PM6. Additionally, the F 1s orbital spectra reveal a prominent peak at 685.43 eV in the 0.025 mg/mL PM6 film, indicating the presence of F elements on the PEDOT:PSS/PM6 film. As for the S 2p orbital, minimal change is observed in the S 2p peak before and after PM6

https://doi.org/10.1021/acsapm.4c01309
ACS Appl. Polym. Mater. 2024, 6, 10254−10262

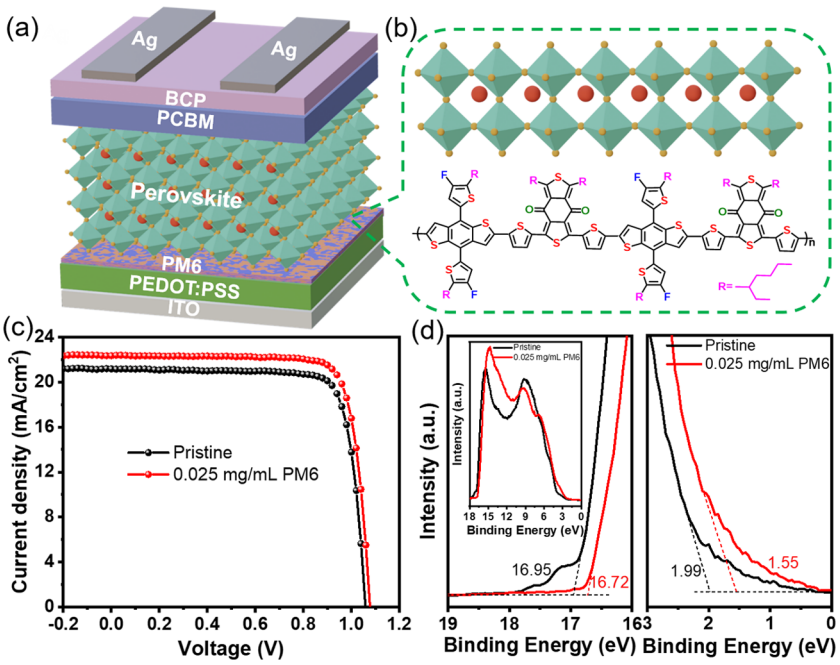

Figure 4. (a) Device structure of a perovskite solar cell. (b) Schematic of the chemical structure and surface passivation of PM6. (c) $J-V$ curves of pristine and 0.025 mg/mL PM6 devices. (d) Light absorption intensity of chalcogenide film.

modification, indicating that PM6 has little effect on both the PEDOT and PSS chains. These XPS analyses collectively highlight the interaction of PM6 with the PEDOT:PSS interface.

SEM was utilized to characterize the surface morphology of the perovskite films, and the influence of various PM6 concentrations on the morphology was investigated. Figures S2a–S2d and Figures 3a and 3b show that after moderate PM6 modification, the presence of PbI_2 (indicated by yellow circles) and holes (indicated by green circles) on the surface of the perovskite film significantly decreases. Additionally, the crystal growth of the perovskite films was measured. The average grain size of the perovskite film modified with 0.025 mg/mL PM6 increased from 448.38 (of the pristine perovskite film) to 530.65 nm, as shown in Figures S3a–S3d. To further investigate the effect of PM6 modication on the perovskite surface roughness, the AFM surface morphologies of the perovskite films were measured. Figures S4a–S4d show that the roughness of the $MAPbI_{3-x}Cl_x$ film on PEDOT:PSS/PM6 gradually increases with higher PM6 concentrations compared to the $MAPbI_{3-x}Cl_x$ film on PEDOT:PSS. The phenomenon of gradual roughness increase is attributed to the increased hydrophobicity of PM6.[15] Hence, optimizing the amount of PM6 added can enhance both the hydrophobicity of PEDOT:PSS and the grain size of the perovskite layer. By promoting charge separation and transport at the PEDOT:PSS/PM6(0.025)/perovskite interface, it reduces interfacial defect recombination and enhances the optoelectronic performance of PSCs.[24]

Furthermore, we assessed the crystalline properties of the perovskite films deposited at various concentrations of PM6 using XRD. As depicted in Figure S5, the diffraction peak at 12.6° corresponds to the (001) crystal plane of residual PbI_2 in the perovskite film, while peaks at 14.2°, 28.5°, and 31.9° correspond to the (110), (220), and (310) crystal planes of the perovskite, respectively. By comparing the diffraction peak signal of the perovskite film at 14.2° deposited on different concentrations of PM6, optimal crystalline properties of the perovskite film were observed at PM6 concentrations of 0.01 and 0.025 mg/mL, as shown in Figure 3c, consistent with the SEM findings. However, upon increasing the PM6 concentration to 0.05 mg/mL, a decrease was observed in the characteristic peak intensity of the perovskite film. This phenomenon was attributed to the heightened hydrophobicity of the ITO/PEDOT:PSS/PM6(0.05) surface, resulting in reduced film quality and crystallinity of the deposited perovskite film.

Next, the study analyzed the ultraviolet–visible absorption spectra of the perovskite layer, as depicted in Figure S6a. PM6, acting as a modification layer for PEDOT:PSS, enhanced the absorption intensity of the perovskite layer, thereby contributing to the improved performance of the inverted PSCs. To further explore the impact of PM6 on carrier transport at the interface, the PL of the PEDOT:PSS/perovskite and PEDOT:PSS/PM6/perovskite films was examined. As illustrated in Figure S6b, under identical testing conditions, the fluorescence intensity at 761 nm of the perovskite films modified with various concentrations of PM6 on PEDOT:PSS was markedly lower than that of the pristine film. This indicates that the modification of PM6 effectively suppressed fluorescence and notably enhanced the hole transport efficiency. However, an increase in the fluorescence intensity of the perovskite film was noted when the PM6 concentration surpassed 0.05 mg/mL. This phenomenon is attributed to the increased hydrophobicity of the substrate, resulting in decreased crystalline quality of the perovskite film (as confirmed by XRD), thus leading to increased interface defects. Here, the PL spectra and absorption spectra of both pristine and 0.025 mg/mL PM6-deposited perovskite films are depicted in Figure 3d.

Thus, we deposited a perovskite light-absorbing layer onto the surface of the PEDOT:PSS/PM6 film. To gain deeper insights into the influence of PM6 on the surface composition of the perovskite, we analyzed the I 3d and Pb 4f spectra of the

https://doi.org/10.1021/acsapm.4c01309
ACS Appl. Polym. Mater. 2024, 6, 10254–10262

perovskite film, as presented in Figures 3e and 3f. From the I 3d orbital spectra, it is clear that the characteristic peaks of I $3d_{5/2}$ and I $3d_{3/2}$ in the PEDOT:PSS/perovskite film are positioned at 618.76 and 630.25 eV, respectively. However, in the PEDOT:PSS/PM6(0.025)/perovskite film, the observed peaks of I $3d_{5/2}$ and I $3d_{3/2}$ are located at 618.45 and 629.95 eV, respectively. Therefore, as a modification layer at the PEDOT:PSS/perovskite interface, PM6 induces a shift of the characteristic peaks of the I element to lower binding energies. Examining the Pb 4f orbitals, it is observed that in the PEDOT:PSS/perovskite film, the characteristic peaks of Pb $4f_{7/2}$ and Pb $4f_{5/2}$ are located at 137.99 and 142.85 eV, respectively. In contrast, in the PEDOT:PSS/PM6/perovskite film, the characteristic peaks of Pb $4f_{7/2}$ and Pb $4f_{5/2}$ are located at 137.84 and 142.70 eV, respectively. Hence, following PM6 modification of PEDOT:PSS, the characteristic peaks undergo a blueshift. Moreover, acting as an intermediate layer at the PEDOT:PSS/perovskite interface, PM6 reduces the presence of metal Pb defects (Pb^0) in the perovskite film. The disappearance of Pb^0 on Pb 4f is attributed to the presence of heteroatoms, such as fluorine (F) and sulfur (S), within the PM6 molecule.[25] Additionally, PM6 improves grain boundary defects and enhances the quality of the perovskite film[26] (supported by SEM images). The improvement reduced energy losses at the interface by facilitating hole extraction and transport across the PEDOT:PSS/perovskite interface, thereby increasing the efficiency of the PSCs.

PSCs were constructed by utilizing the ITO/PEDOT:PSS/PM6/$MAPbI_{3-x}Cl_x$/PCBM/BCP/Ag structure, as illustrated in Figure 4a. The PM6-conjugated polymer incorporates multiple electron-rich functional groups, including thiophene, carbonyl-based, and fluorine groups,[27] as illustrated in Figure 4b. The $J-V$ curves of the PSCs were measured under one sun conditions (100 mW/cm^2, AM1.5 G), as Figure S7a illustrates. The performance characteristics of PSCs with varying concentrations of PM6 modification are compiled in Table 1.

Table 1. Performance Parameters of PSCs with Different PM6 Concentrations

device	V_{oc} (V)	J_{sc} (mA/cm^2)	PCE (%)	FF (%)
pristine	1.04	21.17	18.11	82.27
0.01 mg/mL PM6	1.06	22.53	19.42	81.33
0.025 mg/mL PM6	1.06	22.38	19.46	82.05
0.05 mg/mL PM6	1.06	22.30	19.17	81.07
0.1 mg/mL PM6	1.06	22.29	18.71	79.21

The pristine device exhibited a PCE of 18.11%, a V_{oc} of 1.04 V, a J_{sc} of 21.17 mA/cm^2, and an FF of 82.27%. However, devices based on a 0.025 mg/mL PM6 modification showed the best performance, with a PCE of 19.46%, a V_{oc} of 1.06 V, a J_{sc} of 22.38 mA/cm^2, and an FF of 82.05%, as shown in Figure 4c. Therefore, PM6 as a modification layer for PEDOT:PSS effectively reduces charge recombination and energy losses at the interface between PEDOT:PSS and the perovskite, thereby enhancing the optoelectronic performance of PSCs. However, both the J_{sc} and FF decreased when the concentration of PM6 reached 0.05 mg/mL and higher. This decrease can be attributed to the hydrophobic nature of the excess PM6, which hinders the complete coverage of the perovskite absorber layer on PM6, thereby affecting the rate of charge transport.[28]

UPS tests were conducted on pristine and 0.025 mg/mL PM6 films to assess the impact of the PM6 WF on the device performance. As depicted in Figure 4d, with ultraviolet photons energy at 21.22 eV, the secondary electron cutoff energy in the pristine film was measured at 16.95 eV, corresponding to a WF of −4.27 eV. In contrast, the secondary electron cutoff energy in the 0.025 mg/mL PM6 film was measured at 16.72 eV, corresponding to a WF of −4.50 eV. Consequently, the WF of the PM6(0.025)-modified PEDOT:PSS aligns more closely with that of the perovskite (−5.4 eV). This indicates that the energy difference between PM6(0.025) and the perovskite absorbing layer interface is smaller, thereby reducing the contact barrier and energy loss at the PEDOT:PSS/perovskite interface and ultimately enhancing the V_{oc} of PSCs.[29]

The photovoltaic performance (V_{oc}, J_{sc}, PCE, FF) of 20 distinct PSCs with varying PM6 concentrations is assessed in the study. Devices treated with PM6 exhibit a modest increase in V_{oc} compared to that of unmodified devices, as shown in Figures 5a−5d. This enhancement can be ascribed to the elevated WF of PEDOT:PSS following PM6 modification, which aligns it more closely with the WF of the perovskite absorber layer and thereby reduces the contact barrier between the two materials to minimize energy losses at the interface.[30,31] Additionally, the enhancement in J_{sc} can be credited to the decreased defect density at the PEDOT:PSS/perovskite interface post-PM6 modification, which enhances charge transfer across the interface and improves the collection efficiency of photogenerated charge carriers.[32]

The analysis of photogenerated carrier transport in the solar cell was conducted using the technique of EIS characterization for the PSCs. The Nyquist plots for both the pristine device and the device modified with 0.025 mg/mL PM6 are presented in Figure 6a. Notably, when PM6 is employed to modify PEDOT:PSS, the modified device with 0.025 mg/mL PM6 exhibits a decreased charge transfer resistance (R_{trans}), indicating a faster charge transfer rate at the interface between PEDOT:PSS and the perovskite (as shown in Table S1). We confirmed that using PM6 as a modification layer at the PEDOT:PSS/perovskite interface can effectively mitigate charge recombination, enhance hole extraction and transport rates at the interface, and subsequently improve the optoelectronic performance of PSCs by combining the results of PL and EIS analysis. Furthermore, we assessed the conductivity of the devices using the ITO/PEDOT:PSS/PM6/Ag structure. The results shown in Figure 6a can be further validated by the PM6 modification of PEDOT:PSS, as shown in Figure 6b and Figure S7b, which demonstrates an improvement in the conductivity of the HTL and promotes charge transport.

The SCLC was used to analyze hole-only devices with the structures of ITO/PEDOT:PSS/PM6(0.025)/perovskite/PTAA/Ag to gain deeper insights into the trap density between the PEDOT:PSS/PM6/perovskite interfaces. The graph illustrates two distinct regions: the trap-filled limit zone at high voltages (depicted by the green curve) and the linear Ohmic response region at low voltages (depicted by the blue curve). Notably, as shown in Figure 6c, the onset voltage (V_{TFL}) for the limit zone in the PM6 device is 0.9030 V, which is substantially lower than that of the pristine device (0.9531 V). The following formula was utilized for trap density:

$$N_t = \frac{2\varepsilon_r\varepsilon_0 V_{TFL}}{qL^2} \quad (3)$$

https://doi.org/10.1021/acsapm.4c01309
ACS Appl. Polym. Mater. 2024, 6, 10254−10262

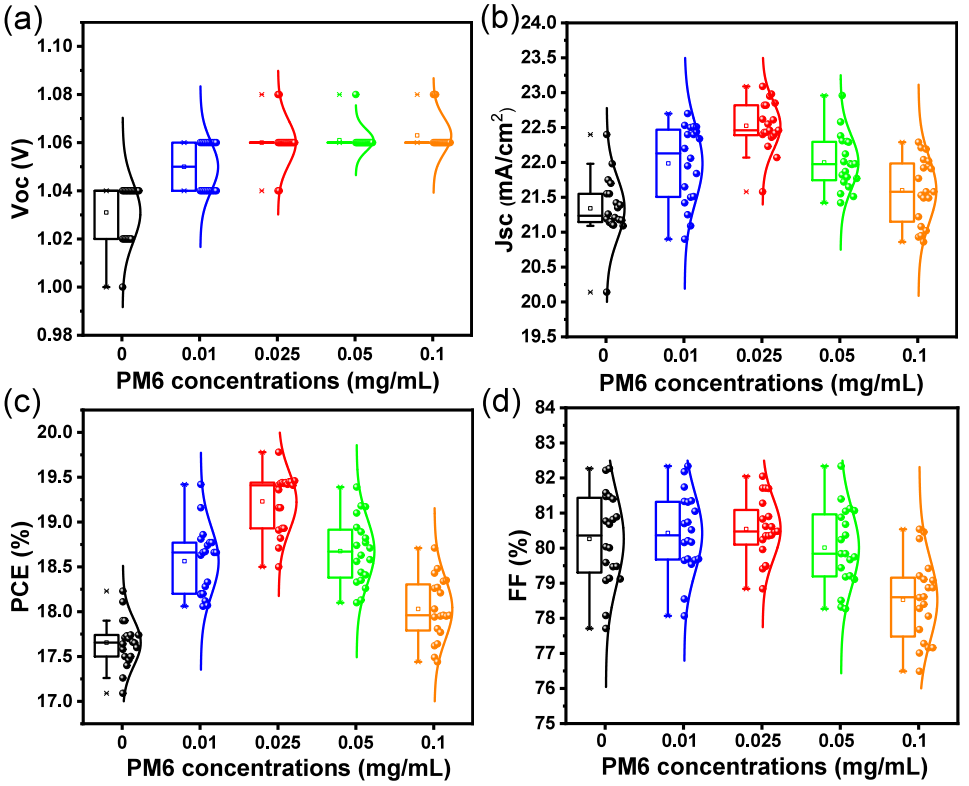

Figure 5. Statistical plots of device performance parameters for different PM6 concentrations: (a) V_{oc}, (b) J_{sc}, (c) PCE, and (d) FF.

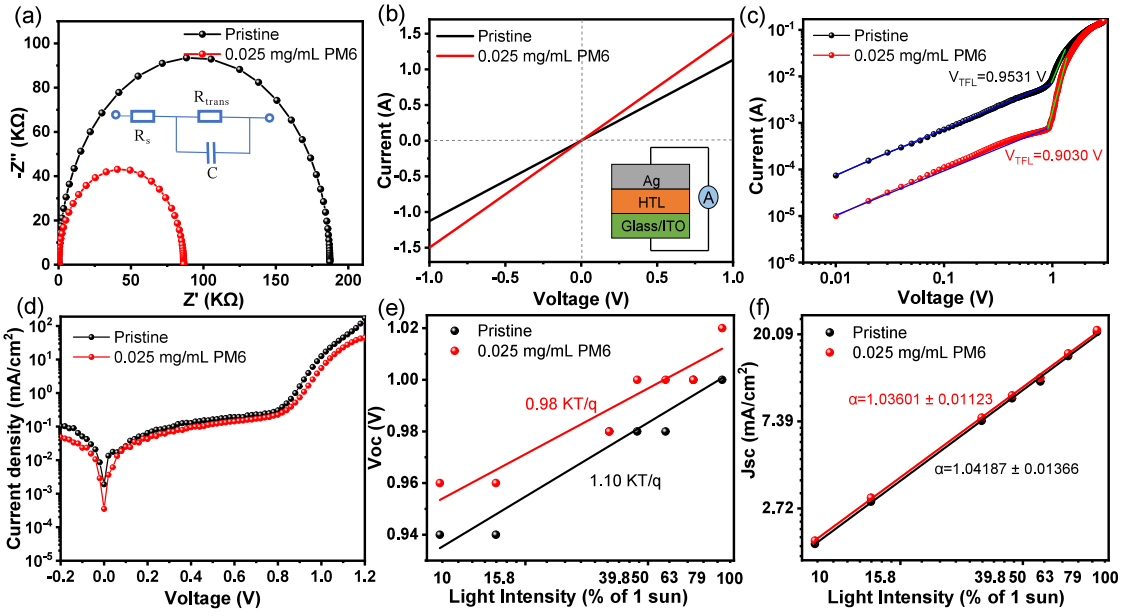

Figure 6. (a) Electrochemical impedance spectroscopy of PSCs. (b) Conductivity of PSCs with the structure glass/ITO/HTL/Ag. (c) J–V curves of hole-only devices with the structure ITO/HTL/perovskite/PTAA/Ag. (d) Dark J–V curves of pristine and 0.025 mg/mL PM6 devices. Battery performance parameters fitted under various light intensities: (e) V_{oc} and (f) J_{sc}.

where N_t represents the trap density, ε_r is the relative permittivity, ε_0 is the vacuum permittivity, q is the elementary charge, and L is the thickness of the perovskite layer. Using the above formula, a significant reduction in the defect density at the interface of the PEDOT:PSS/PM6/perovskite was observed. Subsequently, dark-state J–V curve measurements were performed on the PSCs, as depicted in Figure 6d. It is noteworthy that PSCs modified with PM6 exhibit lower current generation under reverse bias compared to unmodified ones. This can be attributed to the enhanced charge injection capability of PSCs modified with PM6, indicating a reduction in the charge barrier at the interface between the PEDOT:PSS and the perovskite layer. Consequently, PM6-modified PEDOT:PSS can more effectively extract charges.

The ideality factor (n) can qualitatively reflect the density of the defect states in chalcogenide films. In general, the fewer

https://doi.org/10.1021/acsapm.4c01309
ACS Appl. Polym. Mater. 2024, 6, 10254−10262

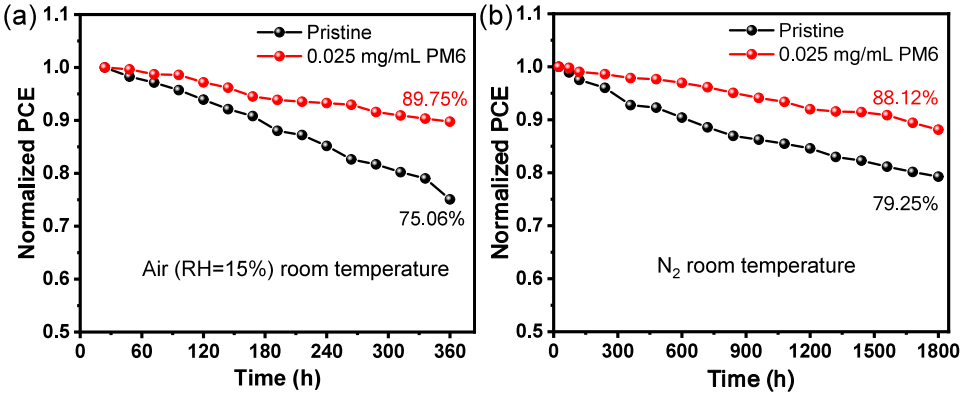

Figure 7. Long-term environmental stability of the PSCs under (a) stability of the device in air (25 °C @ RH 15%) and (b) stability of the device in N_2 (25 °C).

composite or defect states in a device, the lower its ideality factor.[33]

$$n = \frac{q}{K_B T}\frac{\partial V_{oc}}{\partial(\ln \varphi)} \quad (4)$$

where q denotes the elementary charge, T signifies the temperature, K_B stands for the Boltzmann constant, and φ represents the light intensity. Based on the research findings, the device with PM6 as the interface modification layer, as shown in Figure 6e, has an n value of 0.98, whereas the pristine device has an n value of 1.10. As a result, the lower n value indicates that there may be fewer defects at the interface between the perovskite and PEDOT:PSS, Additionally, the impact of light intensity on the current was investigated. As illustrated in Figure 6f, the slope for the PM6-based device (α = 1.036) is nearer to 1 compared to the baseline device (α = 1.042) based on the power-law function $J_{sc} \propto I^{\alpha}$, indicating that with the use of PM6-modified at the interface between PEDOT:PSS and the perovskite, there is less bimolecular recombination.

We analyzed the air stability of both the pristine device and the device modified with 0.025 mg/mL PM6 on PEDOT:PSS in an ambient air environment with a temperature of 25 °C and a relative humidity of 15%. After 360 h, the efficiency of the pristine device had decreased by 75.06%, as shown in Figure 7a. However, the PM6-modified device retained 89.75% of its initial efficiency over the same period. Furthermore, as shown in Figure 7b, stability analysis tests under N_2 encapsulation demonstrated an increased stability for the PM6-modified device, maintaining 88.12% of its initial efficiency after 1800 h. Based on the data presented above, the enhanced stability of PM6-modified devices is attributed partly to the hydrophobic nature of PM6, which prevents degradation of the perovskite film by the PEDOT:PSS layer. Additionally, the modification of PEDOT:PSS by PM6 reduces the roughness of the HTL, resulting in the formation of a denser and higher-quality perovskite film. Therefore, PM6-modified devices exhibit improved stability.

3. CONCLUSIONS

In conclusion, hydrophobic PM6 was utilized in this work as a modification layer for the PEDOT:PSS film interface. The resulting modification enhanced the hydrophobicity and work function of the PEDOT:PSS film and passivated the charge recombination centers on the surface of the perovskite film. This improvement reduced energy losses at the interface by facilitating the extraction and transport of holes at the PEDOT:PSS/perovskite interface. As a result, the PCE of the PSCs increased from 18.11% to 19.46%, and the V_{oc} increased from 1.04 to 1.06 V. Subsequently, the long-term stability of the PSCs was substantially enhanced, with the PCE maintaining 89.75% of its initial value after exposure to air (25 °C @ RH 15%) for 360 h. Therefore, this work demonstrates that modifying the PEDOT:PSS/perovskite interface using PM6 is an effective strategy for enhancing the stability and efficiency of PSCs.

■ ASSOCIATED CONTENT

Supporting Information

The Supporting Information is available free of charge at https://pubs.acs.org/doi/10.1021/acsapm.4c01309.

AFM images of HTL film; SEM and AFM images, XRD, absorption spectra, and steady-state PL of perovskite film; $J-V$ curves of PSCs with different PM6 concentrations; conductivity parameters of the glass/ITO/HTL/Ag device structure; and parameters of an equivalent circuit extracted from the fitting of impedance data (PDF)

■ AUTHOR INFORMATION

Corresponding Authors

Ping Li − *School of Physics and Electronic Science, Zunyi Normal University, Zunyi 563006, China*; Email: lip19870212@126.com

Lijia Chen − *College of Physics and Electronic Engineering, Chongqing Normal University, Chongqing 401331, China*; orcid.org/0009-0001-4539-1354; Email: ljchen01@cqnu.edu.cn

Authors

Yuanlin Yang − *School of Physics and Electronic Science, Zunyi Normal University, Zunyi 563006, China; College of Physics and Electronic Engineering, Chongqing Normal University, Chongqing 401331, China*

Ying Li − *School of Physics and Electronic Science, Zunyi Normal University, Zunyi 563006, China; College of Physics and Electronic Engineering, Chongqing Normal University, Chongqing 401331, China*

Yanqing Yao − *School of Physics and Electronic Science, Zunyi Normal University, Zunyi 563006, China*

https://doi.org/10.1021/acsapm.4c01309
ACS Appl. Polym. Mater. 2024, 6, 10254−10262

Xusheng Zhao − *School of Physics and Electronic Science, Zunyi Normal University, Zunyi 563006, China*
Siwen Wu − *School of Physics and Electronic Science, Zunyi Normal University, Zunyi 563006, China*
Ling Qin − *School of Physics and Electronic Science, Zunyi Normal University, Zunyi 563006, China*
Xiude Yang − *School of Physics and Electronic Science, Zunyi Normal University, Zunyi 563006, China*

Complete contact information is available at: https://pubs.acs.org/10.1021/acsapm.4c01309

Notes

The authors declare no competing financial interest.

■ ACKNOWLEDGMENTS

This work was supported by the National Natural Science Foundation of China (Grants 12264060 and 61874016), the Scientific Research Foundation of Guizhou Province Education Ministry (Grant QJHKYZ [2020]037), the Natural Science Foundation of Chongqing (Grant cstc2021jcyj-msxmX0576), the Scientific and Technological Research Program of the Chongqing Municipal Education Commission (Grant KJQN202200518), and the Doctoral Research Foundation of Zunyi Normal College (Grant ZS-BS [2021]09).

■ REFERENCES

(1) Jiang, Q.; Tong, J. H.; Xian, Y. M.; Kerner, R. A.; Dunfield, S. P.; Xiao, C. X.; Scheidt, R. A.; Kuciauskas, D.; Wang, X. M.; Hautzinger, M. P.; Tirawat, R.; Beard, M. C.; Fenning, D. P.; Berry, J. J.; Larson, B. W.; Yan, Y. F.; Zhu, K. Surface Reaction for Efficient and Stable Inverted Perovskite Solar Cells. *Nature* **2022**, *611* (7935), 278−283.
(2) Liu, C.; Yang, Y.; Chen, H.; Xu, J.; Liu, A.; Bati, A. S. R.; Zhu, H. H.; Grater, L.; Hadke, S. S.; Huang, C. Y.; Sangwan, V. K.; Cai, T.; Shin, D.; Chen, L. X.; Hersam, M. C.; Mirkin, C. A.; Chen, B.; Kanatzidis, M. G.; Sargent, E. H. Bimolecularly Passivated Interface Enables Efficient and Stable Inverted Perovskite Solar Cells. *Science* **2023**, *382* (6672), 810−815.
(3) Zhang, W.; Zhang, T.; Qin, L.; Kang, S.; Zhao, Y.; Li, X. Anti-Solvent Engineering to Rapid Purify PbI_2 for Efficient Perovskite Solar Cells. *Chemical Engineering Journal* **2024**, *479*, No. 147838.
(4) Nyiekaa, E. A.; Aika, T. A.; Orukpe, P. E.; Akhabue, C. E.; Danladi, E. Development on Inverted Perovskite Solar Cells: A review. *Heliyon* **2024**, *10* (2), No. e24689.
(5) Gholami-Milani, A.; Ahmadi-Kandjani, S.; Olyaeefar, B.; Kermani, M. H. Performance Analyses of Highly Efficient Inverted All-Perovskite Bilayer Solar Cell. *Sci. Rep.* **2023**, *13* (1), 8274.
(6) Luo, X. H.; Liu, X.; Lin, X. S.; Wu, T. H.; Wang, Y. B.; Han, Q. F.; Wu, Y. Z.; Segawa, H.; Han, L. Y. Recent Advances of Inverted Perovskite Solar Cells. *Acs Energy Letters* **2024**, *9* (4), 1487−1506.
(7) Wei, J. Y.; Chen, L. J.; Lei, Y. L.; Tan, X. W.; Zhang, Q. M. Improving the Performance of Perovskite Solar Cells with Sodium Stearate-Doped PEDOT:PSS as a Hole Transport Layer. *Acs Applied Polymer Materials* **2024**, *6* (4), 2085−2092.
(8) Ma, S.; Qiao, W. Y.; Cheng, T.; Zhang, B.; Yao, J. X.; Alsaedi, A.; Hayat, T.; Ding, Y.; Tan, Z. A.; Dai, S. Y. Optical-Electrical-Chemical Engineering of PEDOT:PSS by Incorporation of Hydrophobic Nafion for Efficient and Stable Perovskite Solar Cells. *ACS Appl. Mater. Interfaces* **2018**, *10* (4), 3902−3911.
(9) Zhu, C. T.; Gao, J.; Chen, T.; Guo, X. Y.; Yang, Y. Intrinsic Thermal Stability of Inverted Perovskite Solar Cells Based on Electrochemical Deposited PEDOT. *Journal of Energy Chemistry* **2023**, *83*, 445−453.
(10) Ma, S.; Liu, X. P.; Wu, Y. Z.; Tao, Y.; Ding, Y.; Cai, M. L.; Dai, S. Y.; Liu, X. Y.; Alsaedi, A.; Hayat, T. Efficient and Flexible Solar Cells with Improved Stability through Incorporation of a Multifunctional Small Molecule at PEDOT:PSS/Perovskite Interface. *Sol. Energy Mater. Sol. Cells* **2020**, *208*, No. 110379.
(11) Jia, J. B.; Jiang, Z.; Ma, S. Y.; Guo, S. B.; Wu, J. H.; Zhang, Y. Z.; Cao, B. Q.; Dong, J. Novel Strategy for High Efficient and Stable Perovskite Solar Cells through Atomic Layer Deposition. *ACS Appl. Mater. Interfaces* **2024**, *16* (3), 3576−3585.
(12) Chen, T.; Yang, Y.; Zhu, C.; Lin, W.; Dai, Q.; Guo, X. Revealing the Stability Origins of 596 Days-Humidity-Stable Semi-transparent Perovskite Solar Cells. *Journal of Energy Chemistry* **2024**, *94*, 208−216.
(13) Lee, S.; Woo, M. Y.; Kim, C.; Kim, K. W.; Lee, H.; Kang, S. B.; Im, J. M.; Jeong, M. J.; Hong, Y.; Yoon, J. W.; Kim, S. Y.; Heo, K.; Zhu, K.; Park, J. S.; Noh, J. H.; Kim, D. H. Buried Interface Modulation Via PEDOT:PSS Ionic Exchange for the Sn-Pb Mixed Perovskite Based Solar Cells. *Chemical Engineering Journal* **2024**, *479*, No. 147587.
(14) Song, D. H.; Li, H.; Xu, Y. Z.; Yu, Q. M. Amplifying Hole Extraction Characteristics of PEDOT:PSS via Post-treatment with Aromatic Diammonium Acetates for Tin Perovskite Solar Cells. *Acs Energy Letters* **2023**, *8* (8), 3280−3287.
(15) Wang, M.; Wang, H. X.; Li, W.; Hu, X. F.; Sun, K.; Zang, Z. G. Defect Passivation Using Ultrathin PTAA Layers for Efficient and Stable Perovskite Solar Cells with a High Fill Factor and Eliminated Hysteresis. *Journal of Materials Chemistry A* **2019**, *7* (46), 26421−26428.
(16) Al-Gamal, A. G.; Elseman, A. M.; Abdel-Shakour, M.; Chowdhury, T. H.; Kabel, K. I.; Farag, A. A.; Rabie, A. M.; El-Sattar, N.; Fukata, N.; Islam, A. Synergistic effect of integrating N-Functionalized Graphene and PEDOT:PSS as Hole Transporter Bilayer for High-Performance Perovskite Solar Cells. *Advanced Composites and Hybrid Materials* **2023**, *6* (3), 103.
(17) Zhang, Z. L.; Fu, J. F.; Chen, Q. Y.; Zhang, J. J.; Huang, Z. Z.; Cao, J.; Ji, W. X.; Zhang, L. G.; Wang, A. L.; Zhou, Y.; Dong, B.; Song, B. Dopant-Free Polymer Hole Transport Materials for Highly Stable and Efficient $CsPbI_3$ Perovskite Solar Cells. *Small* **2023**, *19* (11), No. 2206952.
(18) Liu, X. H.; Fu, S.; Zhang, W. X.; Xu, Z. X.; Li, X. D.; Fang, J. F.; Zhu, Y. J. A Universal Dopant-Free Polymeric Hole-Transporting Material for Efficient and Stable All-Inorganic and Organic-Inorganic Perovskite Solar Cells. *ACS Appl. Mater. Interfaces* **2021**, *13* (44), 52549−52559.
(19) Gu, W. M.; Jiang, K. J.; Jiao, X. N.; Wu, L. M.; Gao, C. Y.; Fan, X. H.; Yang, L. M.; Wang, Q.; Song, Y. L. Poly(3,4-Ethylenedioxythiophene) as a Hole-Transport Layer for Highly Efficient and Stable Inverted Perovskite Solar Cells. *Chemical Engineering Journal* **2024**, *485*, No. 149512.
(20) Zhang, Z. Y.; Zhang, C.; Liu, W. L.; Zheng, X. M.; Chen, Q. L.; Yang, C. L.; Xu, X. J.; Bo, Z. S. Enhancing the Performance of Organic Solar Cells by Using PDINN-Doped PEDOT:PSS as the Hole Transport Layer. *Polym. Chem.* **2024**, *15* (7), 692−698.
(21) Qiu, F. Z.; Liu, Q. J.; Liu, Y. F.; Wu, J. P. Managing Interface Defects via Mixed-Salt Passivation toward Efficient and Stable Perovskite Solar Cells. *Small* **2023**, *19* (50), No. 2304834.
(22) Luo, H.; Lin, X. H.; Hou, X.; Pan, L. K.; Huang, S. M.; Chen, X. H. Efficient and Air-Stable Planar Perovskite Solar Cells Formed on Graphene-Oxide-Modified PEDOT:PSS Hole Transport Layer. *Nano-Micro Letters* **2017**, *9* (4), 1−11.
(23) Zhu, H. L.; Lin, H.; Song, Z. L.; Wang, Z. S.; Ye, F.; Zhang, H.; Yin, W. J.; Yan, Y. F.; Choy, W. C. H. Achieving High-Quality Sn-Pb Perovskite Films on Complementary Metal-Oxide-Semiconductor-Compatible Metal/Silicon Substrates for Efficient Imaging Array. *ACS Nano* **2019**, *13* (10), 11800−11808.
(24) Alexander, A.; Pillai, A. B.; Pulikodan, V. K.; Joseph, A.; Raees A, M.; Namboothiry, M. A. G. Hydrophobic Poly-TPD Modified PEDOT PSS Surface for Improved and Stable Photovoltaic Performance of $MAPbI_3$ Based p-i-n Perovskite Solar Cells. *J. Appl. Phys.* **2023**, *134* (8), No. 085002.
(25) Fu, Q.; Tang, X. C.; Liu, H.; Wang, R.; Liu, T. T.; Wu, Z. A.; Woo, H. Y.; Zhou, T.; Wan, X. J.; Chen, Y. S.; Liu, Y. S. Ionic Dopant-

Free Polymer Alloy Hole Transport Materials for High-Performance Perovskite Solar Cells. *J. Am. Chem. Soc.* **2022**, *144* (21), 9500−9509.
(26) Wang, L.; Zhang, T.; Yuan, S.; Qian, F.; Li, X.; Zheng, H.; Huang, J.; Li, S. Over 19% Efficiency Perovskite Solar Modules by Simultaneously Suppressing Cation Deprotonation and Iodide Oxidation. *ACS Appl. Mater. Interfaces* **2024**, *16* (4), 4751−4762.
(27) Guo, Q.; Dai, Z.; Dong, C. Q.; Ding, Y. J.; Jiang, N. Z.; Wang, Z. B.; Gao, L.; Duan, C.; Guo, Q.; Zhou, E. R. 17.3% Efficiency $CsPbI_2Br$ Solar Cells by Integrating a Near-Infrared Absorbed Organic Bulk-heterojunction Layer. *Chemical Engineering Journal* **2023**, *461*, No. 142025.
(28) Wang, C. F.; Guo, Y.; Liu, S.; Huang, J. J.; Liu, X. H.; Zhang, J.; Hu, Z. Y.; Zhu, Y. J.; Huang, L. K. Multifunctional Dual-Interface Layer Enables Efficient and Stable Inverted Perovskite Solar Cells. *Phys. Chem. Chem. Phys.* **2024**, *26* (10), 8299−8307.
(29) Sun, Y. S.; Yang, S.; Pang, Z. Y.; Chi, S. H.; Sun, X. X.; Fan, L.; Wang, F. Y.; Liu, X. Y.; Wei, M. B.; Yang, L. L.; Yang, J. H. Hydrogen Tetrachloroaurate-Modulated PEDOT:PSS Film Assembled with Conductive NPB Buffer Layer for High-Performance Planar Perovskite Solar Cells. *Chemical Engineering Journal* **2022**, *432*, No. 134358.
(30) Jiang, K.; Wu, F.; Zhang, G. Y.; Chow, P. C. Y.; Ma, C.; Li, S. F.; Wong, K. S.; Zhu, L. N.; Yan, H. Inverted Planar Perovskite Solar Cells Based on CsI-Doped PEDOT:PSS with Efficiency Beyond 20% and Small Energy Loss. *Journal of Materials Chemistry A* **2019**, *7* (38), 21662−21667.
(31) Zhang, Y. L.; Yu, R. N.; Li, M. H.; He, Z. W.; Dong, Y. M.; Xu, Z. Y.; Wang, R. Y.; Ma, Z. W.; Tan, Z. N. Amphoteric Ion Bridged Buried Interface for Efficient and Stable Inverted Perovskite Solar Cells. *Adv. Mater.* **2024**, *36* (1), No. 2310203.
(32) Liu, B. B.; Zhou, Q.; Li, Y.; Chen, Y.; He, D. M.; Ma, D. Q.; Han, X.; Li, R.; Yang, K.; Yang, Y. G.; Lu, S. R.; Ren, X. D.; Zhang, Z. F.; Ding, L. M.; Feng, J.; Yi, J. H.; Chen, J. Z. Polydentate Ligand Reinforced Chelating to Stabilize Buried Interface toward High-Performance Perovskite Solar Cells. *Angew. Chem., Int. Ed.* **2024**, *63* (8), No. e202317185.
(33) Lin, X. S.; Wang, Y. B.; Su, H. Z.; Qin, Z. Z.; Zhang, Z. Y.; Chen, M. J.; Yang, M.; Zhao, Y.; Liu, X.; Shen, X. Q.; Han, L. Y. An In-Situ Formed Tunneling Layer Enriches the Options of Anode for Efficient and Stable Regular Perovskite Solar Cells. *Nano-Micro Letters* **2023**, *15* (1), 10.

https://doi.org/10.1021/acsapm.4c01309
ACS Appl. Polym. Mater. 2024, 6, 10254−10262